

Unconstrained bending and springback behaviors of aluminum-polymer sandwich sheets

Jianguang Liu^{1,2} · Wei Xue²

Received: 9 July 2016 / Accepted: 21 November 2016 / Published online: 12 December 2016
© Springer-Verlag London 2016

Abstract The bending and springback behaviors of sandwich sheets are more complicated than those of monolithic layer metallic sheet due to the extremely large difference in mechanical properties and in the gauges of polymer core and the skin sheet. In the present study, the bending and springback behaviors of aluminum-polymer sandwich sheets were investigated by using analytical method and conducting experiments and numerical simulations. A simplified analytical model was proposed to calculate the bending moments for sandwich sheet in unconstrained bending process through analyzing the strain and stress distributions of skin sheet and core materials. Then, the analytical model was applied to predict the springback of sandwich sheets after bending. Numerical simulations and experiments of unconstrained bending process for aluminum-polymer sandwich sheets were conducted to investigate the influences of mechanical properties of each layer and thickness ratio of two layers on the folding defects, neutral layer location, and springback. The results show that the neutral layer shifts dramatically toward the compression region of the specimen during bending. The folding angle mainly relates to the strength difference between the skin sheet and the core polymer. The springback angle of sandwich sheet is mainly determined by the mechanical properties of skin sheet.

Keywords Bending · Springback · Sandwich sheet · Aluminum · Polymer

1 Introduction

Metal-plastic sandwich sheet, which consists of two metallic sheet skins with a thermoplastic core in between, is one of the mostly used sandwich sheets [1]. Typically the metallic skin is steel or aluminum alloy and the thermoplastic core is polypropylene or polyethylene. Compared with monolithic metallic sheet, metal-plastic sandwich sheets offer lower density, higher specific flexural stiffness, better dent resistance, and better sound and vibration damping characteristics [2]. Due to these advantages, metal-plastic sandwich sheets are gaining increasing applications in aeronautical, marine, automotive, and civil engineering. Taking automobile industry as example, metal-plastic sandwich sheets have been used to manufacture some automotive components which were formed by the monolithic metallic sheets in order to reduce the weight of the whole car, such as dash panel, wheel house inner, and so on [3].

Aluminum-polymer sandwich sheets have better mechanical properties than steel-plastic sandwich sheets [4]. By using different kinds of aluminum alloy as skin sheet and different kinds of polymer as core, several aluminum-polymer sandwich sheets have been developed [5–9]. Among these aluminum-polymer sandwich sheets, AA5182/polypropylene/AA5182 sandwich sheet has been developed for potential application on automotive body panels in future high performance automobiles with significant weight reduction [10].

The forming of aluminum-polymer sandwich sheets has become a major challenge due to the extremely large difference in mechanical properties and in the gauges of polymer core and the aluminum skins. The forming behaviors of sandwich sheets are quite different from those of monolithic metallic sheets because the interface stress between skin sheet

✉ Jianguang Liu
liujg@hit.edu.cn

¹ Beijing Key Laboratory of Civil Aircraft Structures and Composite Materials, Beijing Aeronautical Science and Technology Research Institute of COMAC, Beijing 102211, People's Republic of China

² School of Materials Science and Engineering, Harbin Institute of Technology, Harbin 150001, People's Republic of China

and core layer has a great influence on the deformation behavior of sandwich sheet [11]. Furthermore, the sliding and shearing behaviors occur between skin sheet and core polymer hence affects the formability of the sandwich sheet. On one hand, the polymer core has a beneficial effect on the forming limit diagram (FLD) of sandwich sheets and the formabilities of sandwich sheets increase with increasing thickness of polymer core [6, 8, 9]. On the other hand, some defects, which do not arise in forming monolithic aluminum sheet, will occur in forming aluminum-polymer sandwich sheets. For example, in the bending process, large deformation in the polymer core causes reverse bending of sandwich sheets at the bent flange [12]. In deep drawing process, the polymer core has negative effect on limit drawing ratio of sandwich sheets because the soft polymer core imposes higher tensile hydrostatic stress on outer aluminum face sheet near punch nose, which causes void volume fraction to increase [13].

Bending is one of the most commonly used sheet metal-forming methods and springback refers to the elastic recovery caused by the release of the non-uniformly distributed stress in a deformed part after the deformation load is removed. Springback significantly affects the geometry accuracy of deformed parts. There have been considerable previous researches on the principle of springback and many methods have been developed to predict the unloading springback of sheet metals, including analytical [14], semi-analytical [15], numerical [16], and other methods [17, 18]. Some factors affecting springback such as mechanical properties, tooling geometry and shape, process parameters, etc., have been widely studied. But most of these researches are for monolithic metallic sheet. In case of springback of sandwich sheets, researches are minor.

Some investigations on springback of metal-plastic sandwich sheets have been conducted in V-, pure, or double curve bending processes. Bending and springback theory of metal-plastic sandwich sheets was firstly developed by Ito et al. [19]. They calculated stress-strain relations and the shift in neutral layer after bending of a sandwich beam and then presented the springback of laminates. After that, some analytical methods have been developed. Liu et al. [20] proposed an analytical solution based on the Euler-Bernoulli straight and curved beam deflections to predict springback and side wall curl for steel/polymer/steel laminates in wiper die bending. Yuen [21] derived a generalized solution for the springback of a multi-layer strip by examining the evolution of the stresses and strains involved in each layer during a stretch bending operation. They then proposed the simplified closed-form solutions for a three-layer composite. Other than developing analytical model, finite element method also has been used to study the bending behaviors and springback for sandwich sheets [12, 22, 23]. Bending moment, sheet thinning, and transverse stress distributions were studied for different punch radii. Results introduced that bending moment distribution, which

directly affects springback, is dependent on punch radius, contact pressure, sheet thinning, and relative sheet-die geometry [24]. Springback increases with punch stroke, punch radius, and die opening in air-bending process, and die opening was found to be the most influential parameter [25]. Springback also increases with increasing friction coefficient and core thickness, and decreases the bending radii in double curve bending process [26]. Bending at elevated temperatures led to a reduced springback in both four-point bend and channel bend tests [27].

In this paper, the bending and springback behaviors of aluminum-polymer sandwich sheets were systemically investigated by using analytical method and conducting experiments and numerical simulations. A simplified analytical model was proposed to calculate the bending moments for sandwich sheets in unconstrained bending process through analyzing the strain and stress distributions of skin sheet and core materials. Then, the analytical model was applied to predict the springback after bending. Numerical simulations and experiments of unconstrained bending processes for aluminum-polymer sandwich sheets were conducted to investigate the influences of structure parameters and mechanical properties of sandwich sheets on the reverse bending, neutral layer shift, and springback.

2 Analytical analysis of springback

The structure of sandwich sheet is shown in Fig. 1. It consists of two layers of metallic sheet as skin and a polymeric material as core. Rule-of-mixtures (ROM), based on volume fraction of metal and polymer layers in the laminate, was used to predict the Young's modulus and Poisson's ratio of sandwich sheets.

$$t_s = 2t_f + t_c \quad (1)$$

$$E_s = (2E_f t_f + E_c t_c) / t_s \quad (2)$$

$$\mu_s = (2\mu_f t_f + \mu_c t_c) / t_s \quad (3)$$

where E , μ , and t are the Young's modulus, Poisson's ratio, and thickness, respectively. Subscript s , f , and c denote sandwich sheet, metallic skin sheet, and polymer core.



Fig. 1 The structure of sandwich sheet

The schematic view of sandwich sheet-bending model is shown in Fig. 2. In the figure, R_i and R_o are radii of concave and convex surfaces, respectively. R_n is the neutral layer radius. R_c is the central surface radius. θ is the bending angle. In order to calculate the bending moment, some basic assumptions for sandwich sheet-bending are listed here:

1. The plane section remains planar during bending with the prescribed tensile force.
2. The strain due to bending is proportional to the distance from the neutral layer.
3. The neutral layer is a zero-strain layer.
4. Straight lines perpendicular to the neutral layer remain straight during the bending process of sandwich sheets.
5. Bauschinger effect is neglected and only elastic deformation occurs during the unloading process for metallic sheet.
6. The shear stress at the interface of metallic sheet and polymer core is ignored.
7. The sandwich sheet is wide enough relative to its thickness. Therefore, the strain in the width direction is zero.
8. Ignoring the through-the-thickness compression and then the through-the-thickness stress is zero.

Basing on these assumptions, the bending moments were derived in the following sections.

2.1 Stress in the section of sandwich sheet

Figure 3 shows the strain and stress distributions in transverse direction through-the-sandwich sheet thickness under bending. Where h is the distance from the inner surface of outer metallic sheet to the neutral layer. h_1 is the elastic region thickness of outer metallic sheet, and h_2 is the elastic region thickness of inner metallic sheet. The bending deformation of sandwich sheet can be divided into six portions: elastic tensile region and elastic compressive region in polymer core, elastic tensile region in outer metallic sheet, elastic compressive region in inner metallic

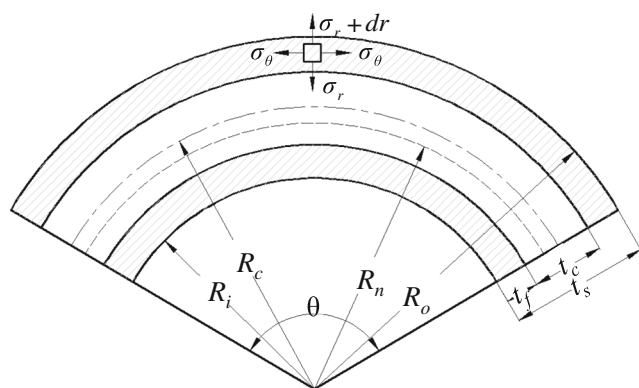


Fig. 2 Schematic view of the sandwich sheet-bending model

sheet, elasto-plastic tensile region in outer metallic sheet, and elasto-plastic compressive region in inner metallic sheet.

The calculations of stress and corresponding moment at each portion were derived as follows:

Based on Kirchhoff theory, the bending strain can be approximated as

$$\varepsilon_\theta = \frac{R-R_n}{R_n} \tag{4}$$

Due to the small deformation degree of core polymer and that the strain at the elastic limit of the polymer is much larger than that for the metal, the elastic deformation behavior with no viscous effect is considered for the core polymer. The elastic region of polymer follows Hooke’s law and the stress in transverse direction can be expressed as

$$\sigma_\theta = \frac{E(R-R_n)}{(1-\mu^2)R_n} \tag{5}$$

where σ_θ denotes the stress in transverse direction.

During bending process, the skin sheet may undergo elastic, elasto-plastic, or full plastic deformations. It depends on the thickness of core polymer and the yield stress of aluminum alloy sheet. When the sandwich sheet is very thin and the bending radius is relatively large, the skin sheet undergoes elastic deformation and the bending angle will completely recover after unloading. For this case, the springback angle do not need to be calculated. When the sandwich sheet is very thick and the bending radius is relatively small, the skin sheet will partially or completely undergo plastic deformation and then the bending angle will partially recover after unloading.

According to Hill’s quadratic yielding function, for anisotropic skin sheet, the material yields

$$F^2(\sigma_{ij}, \varepsilon_{ij}) = \sigma_\theta^2 + \sigma_z^2 - \frac{2\bar{r}}{1+\bar{r}}\sigma_\theta\sigma_z - \bar{\sigma}^2 = 0, \tag{6}$$

where $\bar{\sigma}$ is the equivalent stress, σ_z is the width stress, and \bar{r} is the transverse anisotropy coefficient.

Because the plastic strain in transverse direction is zero, so that

$$d\varepsilon_z^p = d\lambda \frac{\partial F}{\partial \sigma_z} = 0, \tag{7}$$

where $d\lambda$ is a coefficient relative to a material hardening rule.

Combined with Eq. (6), σ_z can be expressed as

$$\sigma_z = \frac{\bar{r}}{1+\bar{r}}\sigma_\theta. \tag{8}$$

Substitution of Eq. (8) into Eq. (6) yields

$$\sigma_\theta = f\bar{\sigma}, \tag{9}$$

where

$$f = \frac{1 + \bar{\epsilon}}{\sqrt{1 + 2\bar{\epsilon}}}.$$

From plastic work formulation, the equivalent strain is

$$\bar{\epsilon} = f \epsilon_{\theta}. \quad (10)$$

Assuming that the plastic region material of aluminum alloy sheet follows exponential strain hardening law, namely:

$$\bar{\sigma} = k \left(\epsilon_0 + \bar{\epsilon} \right)^n, \quad (11)$$

where $\bar{\epsilon}$ is the equivalent plastic strain. k is the strength coefficient. n is strain hardening index, and ϵ_0 is the initial strain.

Substitution of Eqs. (9) and (10) into Eq. (11), the transverse stress in skin layer is

$$\sigma_{\theta} = kf \left(\epsilon_0 + f \frac{R - R_n}{R_n} \right)^n. \quad (12)$$

2.2 Bending moments

The bending moments of sandwich sheet at the end of the loading process are the summation of bending moments in three layers,

$$M_s = M_{if} + M_c + M_{of}, \quad (13)$$

where M_s is the total bending moment of sandwich sheet, M_{if} is the bending moment of inner layer aluminum alloy sheet, M_c is the bending moment of core polymer, and M_{of} is the bending moment of outer layer aluminum alloy sheet.

During the bending process of sandwich sheets, the neutral layer locates near the inner surface. The deformation in inner skin sheet is different from that in outer skin sheet. The location of the neutral layer is expressed by the distance between the neutral layer and the outer surface h . The bending moment of each layer can be derived according to the stress distribution.

1. Bending moment of core polymer

The bending moment of core polymer can be calculated by integrating the elastic stress multiplied by the coordinate from the neutral layer.

$$M_c = \int_{h-t_c}^h \sigma_{\theta} y dy = \frac{E_c}{3R_n(1-\mu_c^2)} \left[h^3 - (h-t_c)^3 \right] \quad (14)$$

2. Bending moment of skin sheet

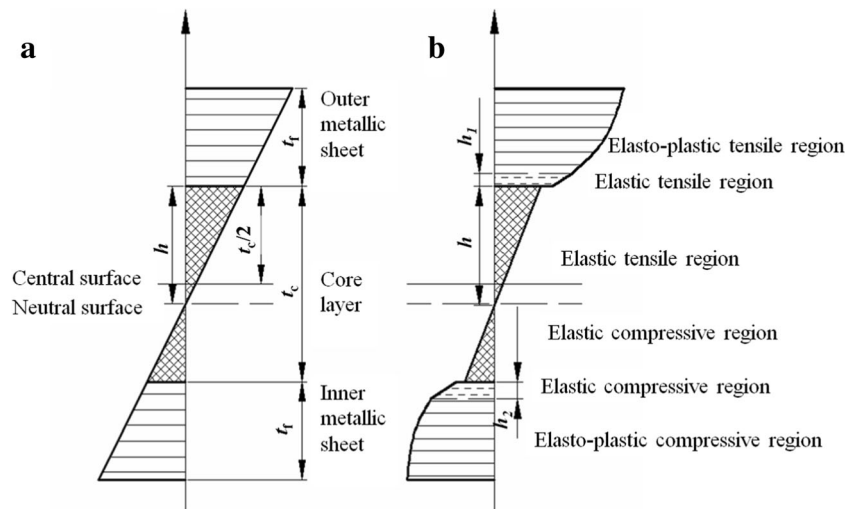
Assuming the skin sheet undergoes elasto-plastic deformation, the bending moment of outer skin sheet can be determined as

$$\begin{aligned} M_{of} &= \int_h^{h+h_1} \frac{E_f}{(1-\mu_f^2)} y^2 dy + \int_{h+h_1}^{h+t_f} kf \left(\epsilon_0 + f \frac{y}{R_n} \right)^n y dy \\ &= \frac{E_f}{3R_n(1-\mu_f^2)} \left[(h+h_1)^3 - h^3 \right] + \frac{kR_n}{n+1} \left(\epsilon_0 + f \frac{h+t_f}{R_n} \right)^{n+1} (h+t_f) - \frac{kR_n}{n+1} \left(\epsilon_0 + f \frac{h+h_1}{R_n} \right)^{n+1} (h+h_1) - \\ &\quad \frac{kR_n^2}{(n+1)(n+2)f} \left(\epsilon_0 + f \frac{h+t_f}{R_n} \right)^{n+2} + \frac{kR_n^2}{(n+1)(n+2)f} \left(\epsilon_0 + f \frac{h+h_1}{R_n} \right)^{n+2}. \end{aligned} \quad (15)$$

The bending moment of inner skin sheet can be determined as

$$\begin{aligned} M_{if} &= \int_{t_c-h}^{t_c-h+h_2} \frac{E_f}{(1-\mu_f^2)} y^2 dy + \int_{t_c+h_2-h}^{t_c+t_f-h} kf \left(\epsilon_0 + f \frac{y}{R_n} \right)^n y dy \\ &= \frac{E_f}{3R_n(1-\mu_f^2)} \left[(t_c-h+h_2)^3 - (t_c-h)^3 \right] + \frac{kR_n}{n+1} \left(\epsilon_0 + f \frac{t_c+t_f-h}{R_n} \right)^{n+1} (t_c+t_f-h) - \frac{kR_n}{n+1} \left(\epsilon_0 + f \frac{t_c+h_2-h}{R_n} \right)^{n+1} (t_c+h_2-h) - \\ &\quad \frac{kR_n^2}{(n+1)(n+2)f} \left(\epsilon_0 + f \frac{t_c+t_f-h}{R_n} \right)^{n+2} + \frac{kR_n^2}{(n+1)(n+2)f} \left(\epsilon_0 + f \frac{t_c+h_2-h}{R_n} \right)^{n+2}. \end{aligned} \quad (16)$$

Fig. 3 a Transverse strain and **b** transverse stress distributions in the sandwich sheet thickness under bending



Bending moments are discussed for two conditions.

1. When $h_1 = 0$, the first term in Eq. (15) will be zero and then the bending moment of outer skin sheet is a fully plastic moment. When $h_1 = t_f$, other terms except the first term will be zero and then the bending moment of outer skin sheet is a fully elastic moment.
2. For inner skin sheet, when $h_2 = 0$, the bending moment of inner skin sheet is a fully plastic moment. When $h_2 = t_f$, the bending moment of inner skin sheet is a fully elastic moment.

h_1 and h_2 are derived as the following expressions:

$$h_1 = \frac{f\bar{\sigma}_s R_n (1 - \mu_f^2)}{E_f} - (R_i + t_f + t_c - R_n), \tag{17}$$

$$h_2 = \frac{f\bar{\sigma}_s R_n (1 - \mu_f^2)}{E_f} + (R_i + t_f - R_n). \tag{18}$$

2.3 Calculation of springback angle

The non-uniform stress distributions through sheet thickness during bending process will change the part profile and cause springback when the loading is removed. Figure 4 shows the schematic view of springback angle and folding angle.

After calculating the moment, the springback angle can be calculated by

$$\Delta\theta = \frac{12M_T}{\bar{E}t^3}, \tag{19}$$

where $\Delta\theta$ is springback angle, t is thickness of sheet, \bar{E} is plane strain Young’s modulus, expressed as

$$\bar{E} = \frac{E}{1 - \mu^2}, \tag{20}$$

During the unloading process, the recovery of shear stress in sandwich sheet will result in the changing of shape and dimension. The moment acts in an opposite sense and changes the curvature radius of the neutral layer.

$$\frac{1}{R_n} - \frac{1}{R'_n} = \frac{M_s}{E_s I_s}, \tag{21}$$

where R'_n is the curvature radius of the neutral layer after unloading and I_s is the area moment of inertia per unit width of sandwich sheet, expressed as

$$I_s = \frac{(2t_f + t_c)^3}{12}. \tag{22}$$

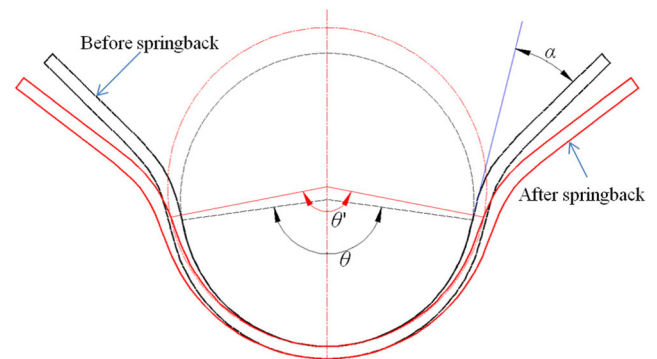


Fig. 4 Measurement of bending angle and folding angle before and after springback

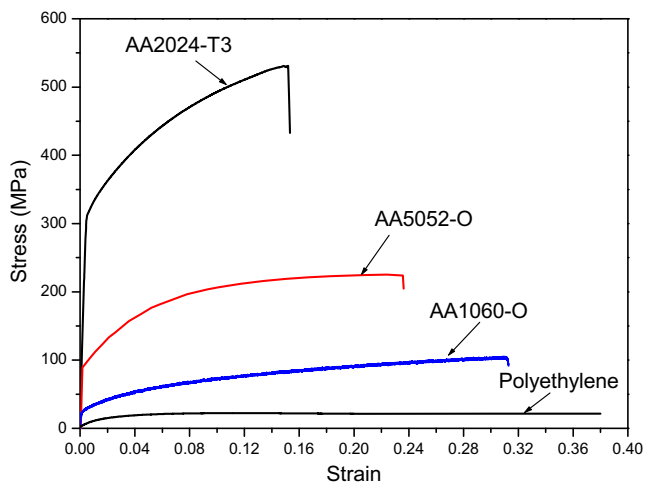


Fig. 5 Strain-stress curves of aluminum alloy sheets and polyethylene

E'_s is the Young's modulus of sandwich sheet under plane strain state, expressed as

$$E'_s = \frac{E_s}{1-\mu_s^2}. \quad (23)$$

At the end of the unloading process, the radius of the neutral layer can be determined by using the equation

$$R'_n = \frac{(2t_f E_f + t_c E_c)(2t_f + t_c)^2 R_n}{(2t_f E_f + t_c E_c)(2t_f + t_c)^2 - 12M_s R_n}. \quad (24)$$

Assuming that the end of sandwich sheet keeps plane before and after unloading, the bending angle before unloading θ and the angle after unloading θ' can be determined. So

$$R'_n \theta' = R_n \theta. \quad (25)$$

After bending, the specimens were removed from the tool and the angle changes were measured. The springback angle $\Delta\theta$ of sandwich sheet after unloading can be determined by solving Eq. (26).

$$\Delta\theta = \theta - \theta' \quad (26)$$

Table 1 Mechanical properties of aluminum alloy sheets and polyethylene

| Materials | AA5052-O | AA2024-T3 | AA1060-O | Polyethylene |
|---------------------------------|----------|-----------|----------|-----------------|
| Young's modulus, E (GPa) | 69 | 66.7 | 69 | 0.8 |
| Poisson's ratio, μ | 0.33 | 0.33 | 0.33 | 0.42 |
| Yield stress, σ_s (MPa) | 108 | 335 | 22 | Shown in Fig. 5 |
| Strength coefficient, k (MPa) | 428.9 | 814 | 152.81 | |
| Strain hardening index, n | 0.28 | 0.245 | 0.325 | |
| Normal anisotropy exponent, r | 0.69 | 0.9 | 1.0 | – |

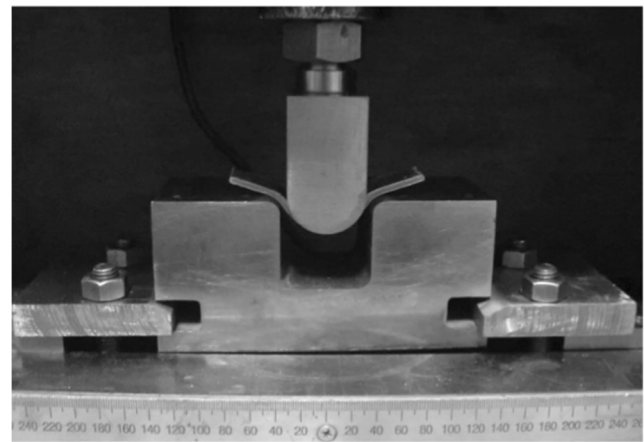


Fig. 6 Unconstrained cylindrical bending test equipment

3 Unconstrained bending experiments of sandwich sheets

3.1 Sandwich sheets

Three commonly used structure aluminum alloy (AA1060-O, AA2024-T3, and AA5052-O) were used as skin sheet of sandwich sheets. Its thickness is 0.5 mm. The thickness of polyethylene are 0.5, 1.0, and 2.0 mm, respectively. Tensile tests were conducted to determine mechanical properties of aluminum alloy and polyethylene according to ASTM-E8 standard. The engineering strain-nominal stress curves of aluminum alloy sheets and polyethylene are shown in Fig. 5. The plastic behavior of aluminum alloy sheet was described by using a Swift-type hardening law (Eq. (11)). Table 1 lists the mechanical properties of these three aluminum alloys and polyethylene sheet. Compared with metallic sheet, polyethylene has a larger elastic deformation zone. Aluminum-polyethylene sandwich sheets were fabricated by hot press bonding [8]. A 50- μm -thick layer of a hot-melt adhesive was inserted between polyethylene sheet and aluminum alloy sheet. Then, the sandwich sheet was consolidated by heating to 180 °C in a hot press for 7–10 min. The thickness of sandwich sheets was measured after fabrications.

3.2 Unconstrained bending tests

Unconstrained cylindrical bending tests were conducted to investigate the springback for all sandwich sheets. Three specimens as a group were tested to check the scatter of experimental results. The cylindrical bending tests were carried out on a universal testing machine. Figure 6 illustrates the experimental setup. The punch is connected with the movable crosshead. The velocity of bending punch is set to move in a speed of 3 mm/min to reach the expected stroke depth of 25 mm. The radius of punch is 17 mm. The load cell measured the bending force. Before experiments, specimens with 100-mm length and 25-mm width were prepared. The bent samples were then removed from the tooling and their angles after springback were measured. Experimental samples after bending tests are shown in Fig. 7. To measure the bending angles of the test samples before and after springback, images were taken using a digital camera. Then, the angles from the images taken before springback (Fig. 6) and after springback (Fig. 7) were measured using CAD software.

4 Numerical analysis of unconstrained bending and springback of sandwich sheets

4.1 Finite element analysis model

Several approaches have been proposed to model the sandwich sheets. The simplest method is to consider the sandwich sheets as a homogeneous material using the overall tensile properties of the sandwich sheet. But this method cannot account for the deformation difference between skin material and core material. In the present study, the commercial FEA software package ABAQUS/Standard was used to simulate the bending and unloading process of sandwich sheets. A three-layer sandwich sheet with skin sheet of aluminum alloy and central sheet of polymer was constructed. The adhesion behaviors at the interface of skin sheet and core polymer were ignored because debonding seldom occurs in bending process for sandwich sheet. The 4-node bilinear plane stress quadrilateral, reduced integration element, CPS4R, is used to model the bending sample. In the numerical simulations, frictional effects were taken into account by means of the Coulomb model. The friction coefficients between punch and sandwich sheet and sandwich sheet and die were set to 0.05, in order to

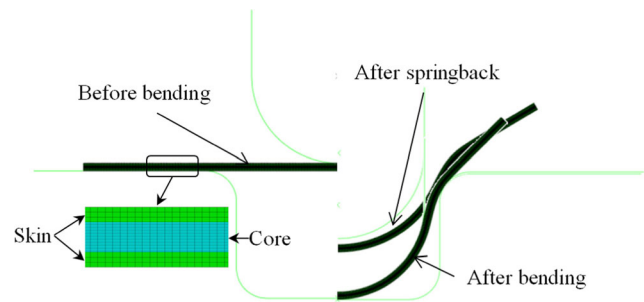


Fig. 8 Finite element analysis model of unconstrained bending test

simulate the utilization of lubricants. Figure 8 shows the finite element model of unconstrained cylindrical bending tests. Taking into account the plane and symmetrical deformation of bending sample, only a sectional half model was set up. The process parameters in numerical simulations are same with those in experiments. In order to investigate the influences of core polymer on the bending and springback behaviors, other two polymers were used as core of sandwich sheets. Mechanical properties of these two polymers are listed in Table 2. Among these three polymers, the strength of nylon is the highest and the strength of polyethylene is the lowest. In numerical simulations, thickness of core polymers are 0.5, 1.0, and 1.5 mm, respectively.

4.2 Validation of FEA models

Numerical simulation results were compared with experimental results to validate the used FEA model. Figure 9 shows the punch loads obtained from the simulations for test specimens with different thicknesses and three aluminum alloy skin sheets. The predicted punch loads have good agreements with experimental ones. Then, the used numerical simulation model for sandwich sheet was validated.

5 Unconstrained bending behavior

5.1 Folding angle

During the bending process of sandwich sheets, a folding defect was observed due to the shear deformation produced in the polymeric layer [12]. In Fig. 5, folding defects were seen in some bent specimens. The AA2024-polyethylene

Fig. 7 Bending test samples with the skin sheet of: **a** AA2024, **b** AA5052 and **c** AA1060

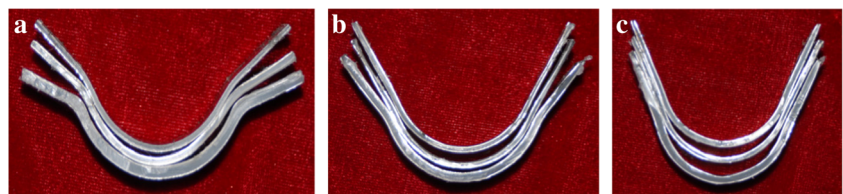


Table 2 Mechanical properties of two polymers

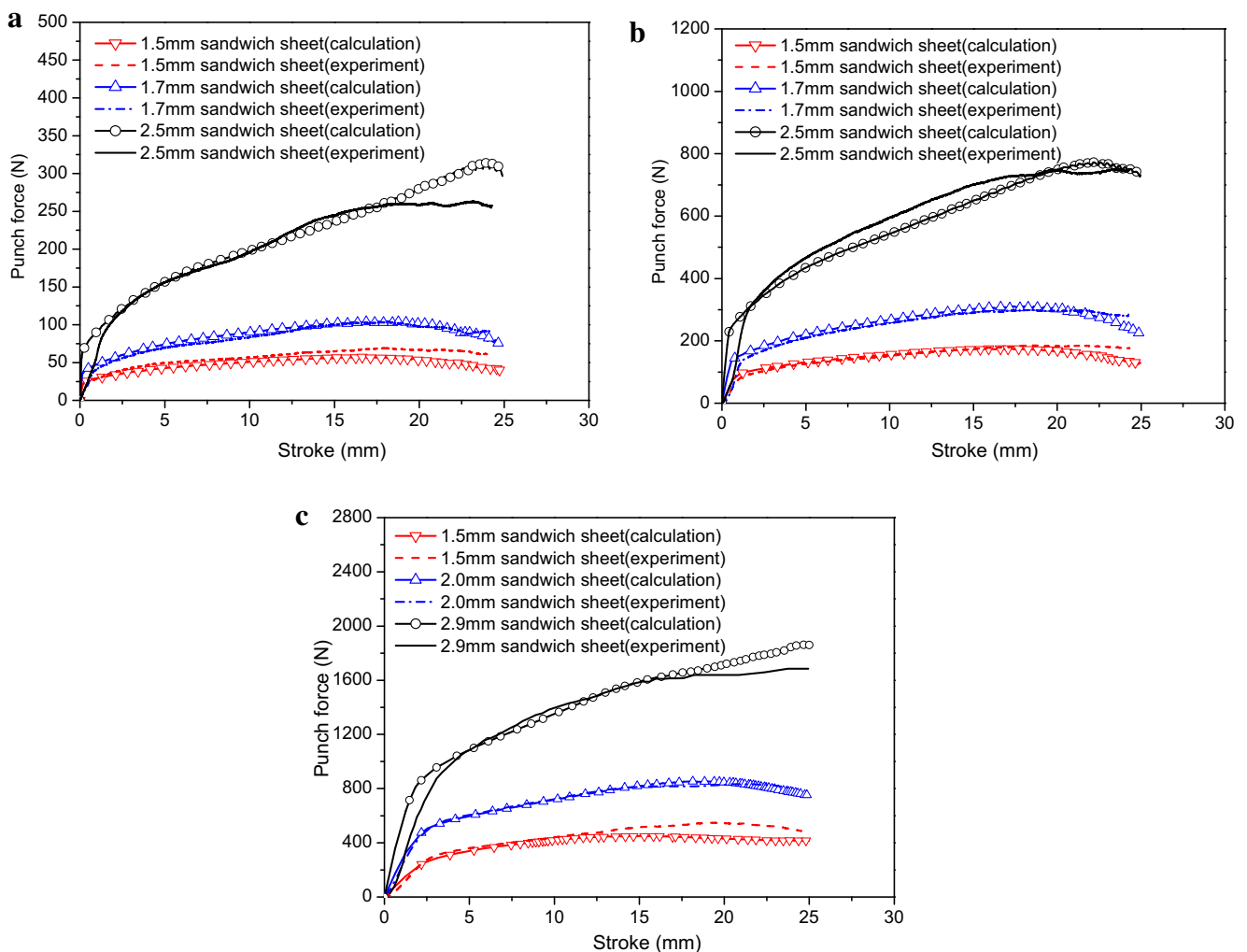
| Materials | Young's modulus E (GPa) | Poisson's ratio ν | Yield stress σ_s (MPa) | Stress-plastic strain relationship (MPa) |
|---------------|---------------------------|-----------------------|-------------------------------|---|
| Nylon-6 | 2.75 | 0.33 | 56.9 | $\bar{\sigma} = 132.4(0.1 + \bar{\epsilon})^{1.6} + 53.6$ |
| Polypropylene | 0.83 | 0.33 | 23.5 | $\bar{\sigma} = 29.4(0.1 + \bar{\epsilon})^{2.0} + 23.25$ |

sandwich sheet with core thickness 1.9 mm shows obviously folding defect. But for AA1060-polyethylene sandwich sheet, no visible folding defects can be seen. In order to investigate the effects of sandwich structure on folding defects, folding angle α of three aluminum alloy sandwich sheets were compared. Figure 10 show the deformed geometries of bent specimens before springback. Table 3 summarizes the folding angle values of all bent specimens. For AA1060 skin sheet, whatever the core polymer is, the folding angle is very small. But for AA2024 skin sheet, the folding angle is very large when the core polymer is polyethylene or polypropylene.

Generally speaking, the folding angle value increases with increasing strength of skin sheet and decreasing strength of core polymer. In other words, the more the strength difference between the skin sheet and the core polymer is larger, the folding angle is bigger. Furthermore, the folding angle also increases with the thickness of sandwich sheet.

5.2 Stress distributions in the sandwich sheet thickness

The stress distribution in a sheet-bending part before unloading decides the magnitude and direction of springback

**Fig. 9** Load-stroke curves of aluminum-polymer sandwich sheets with the skin sheet of **a** AA1060, **b** AA5052, and **c** AA2024

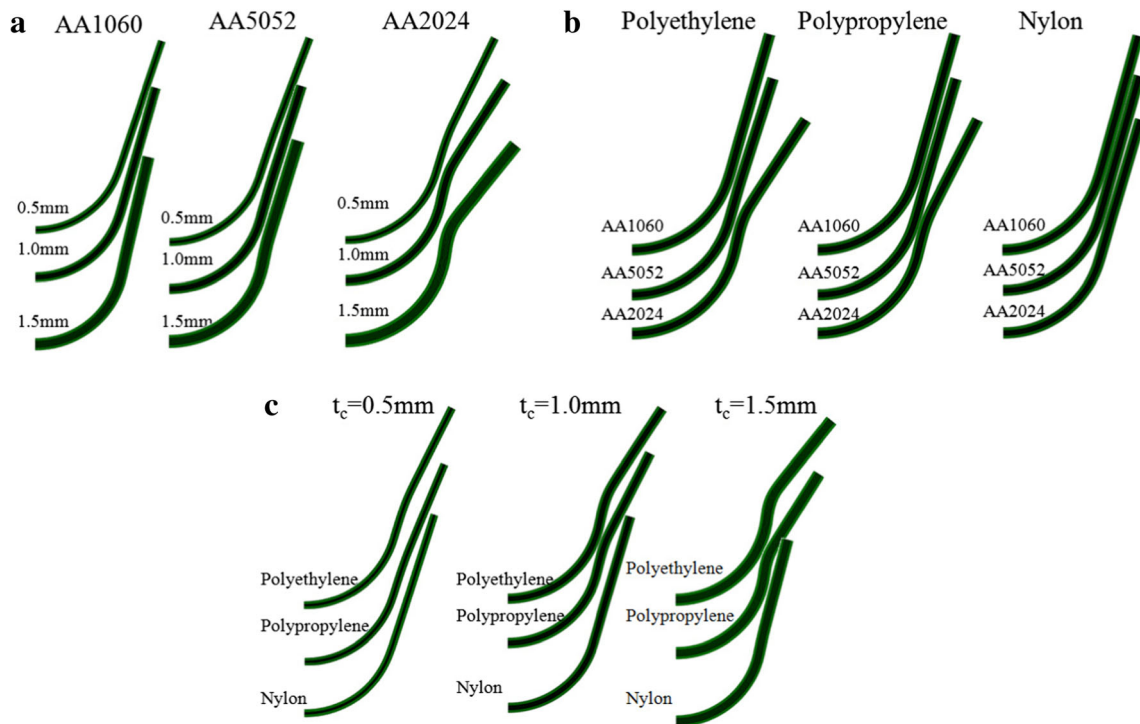


Fig. 10 Deformed geometries of bent specimens before springback for three cases: **a** core polymer = polyethylene, **b** $t_c = 1.0$ mm, and **c** skin sheet = AA2024

of the part after unloading. The transverse stress distributions in the sandwich sheets at the bending zones are presented in Fig. 11 for the following two cases: when the core polymer is polyethylene and when the skin aluminum alloy is AA5052. For the two cases, the thickness of core polymer is 1.0 mm. From Fig. 11a, it can be seen that the transverse stress distributions on the inner and outer face show great difference, but the transverse stress distributions on core polymer are same for the three sandwich sheets. So, skin sheets have no effect on the transverse stress distribution on the core polymer. Figure 11b shows the influence of core polymer on the transverse stress distribution in sandwich sheet thickness. The core

polymer has not effect on the stress distribution of skin sheet but great effect on that of core polymer.

5.3 Location of neutral layer

The location of neutral layer is significant to sandwich sheet and it has an important effect on springback calculation during bending. However, how the neutral layer of sandwich sheet shifts has still not been confirmed. So, the present work aims at understanding the shift of neutral layer of sandwich sheet during bending. Effects of some structure factors of sandwich sheets on the location of neutral layer were analyzed.

1. Mechanical properties of skin sheet

Figure 12 shows the transverse strain distributions for three sandwich sheets and monolithic layer AA5052 aluminum sheet with same thickness of sandwich sheet. For these three sandwich sheets, the core polymer is polypropylene and its thickness is 1.0 mm. The total thickness of sandwich sheet is 2.0 mm. The outer region of the sandwich sheet is under tension state while the inner region is under compression state, which is consistent with monolithic layer metallic sheet. Because the core polymer is thick, the neutral layer lies within the core polymer.

In order to clearly show the effect of skin aluminum alloy sheet on the location of neutral layer of sandwich sheet, the

Table 3 Folding angle values of bent specimens

| Core polymer | Thickness (mm) | Aluminum alloy skin sheet | | |
|---------------|----------------|---------------------------|--------|--------|
| | | AA1060 | AA5052 | AA2024 |
| Polyethylene | 0.5 | 0.45 | 1.539 | 9.147 |
| | 1.0 | 0.982 | 2.309 | 17.756 |
| | 1.5 | 1.54 | 5.202 | 26.86 |
| Polypropylene | 0.5 | 0.312 | 0.989 | 5.423 |
| | 1.0 | 0.41 | 1.036 | 11.671 |
| | 1.5 | 0.683 | 2.547 | 20.451 |
| Nylon | 0.5 | 0.1 | 0.129 | 0.599 |
| | 1.0 | 0.12 | 0.204 | 0.735 |
| | 1.5 | 0.11 | 0.634 | 2.52 |

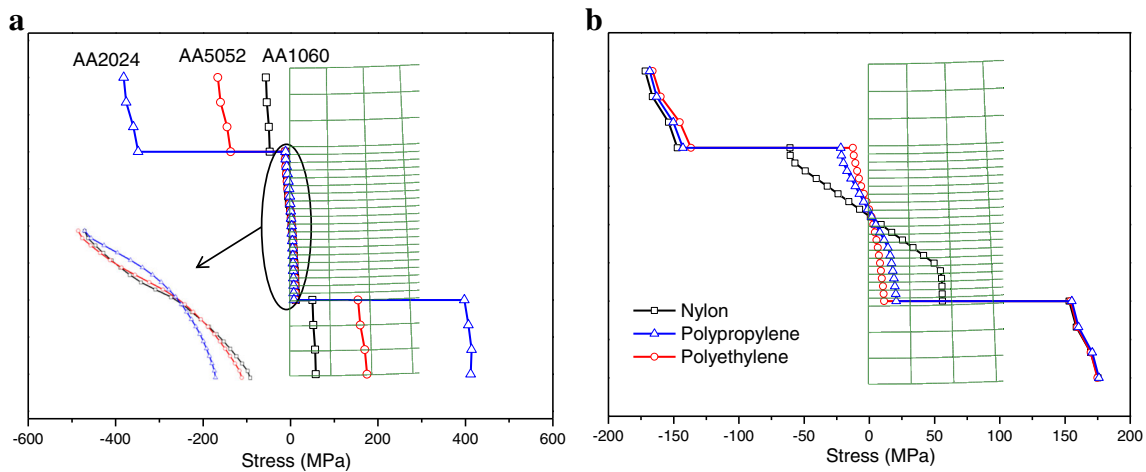


Fig. 11 Transverse stress distributions in sandwich sheets after bending for the case of **a** core polymer = polyethylene and **b** skin sheet = AA5052

neutral layer radius was measured for sandwich sheet and was compared with that of monolithic layer aluminum alloy sheet, as shown in Fig. 13. The analytical neutral layer radius of 5052 aluminum alloy sheet was calculated according to the classical Hill’s theory. The simulated neutral layer radius of 5052 aluminum alloy sheet is 17.954 mm and is almost equal to the analytical value of 17.97 mm. The neutral layer radius of sandwich sheet is smaller than that of 5052 aluminum alloy sheet. For these three sandwich sheets, the neutral layer radius of AA1060-polypropylene is the largest and that of AA2024-polypropylene is the smallest, as shown in Fig. 14. The neutral layer radius of sandwich sheet decreases with increasing strength of aluminum alloy sheet. In other word, the neutral layer shifts to the compression region with increasing strength of aluminum alloy sheet.

2. Mechanical properties of core materials

Next, the influence of core polymers on the location of neutral layer was analyzed. Figure 15 shows the neutral layer radii of sandwich sheets with three core polymers. For these sandwich sheets, the thickness of core polymer is 1.0 mm and the total thickness of sandwich sheet is 2.0 mm. From Fig. 14, it can be seen that the core polymer has a great effect on the location of neutral layer. The neutral layer radius of aluminum-nylon sandwich sheet is the biggest and that of aluminum-polyethylene sandwich sheet is the smallest. The neutral layer radius increases with increasing strength of core polymer. Furthermore, the strength of core polymer affects the location of neutral layer to a different degree for three aluminum alloy skin sheet. With increasing strength of aluminum

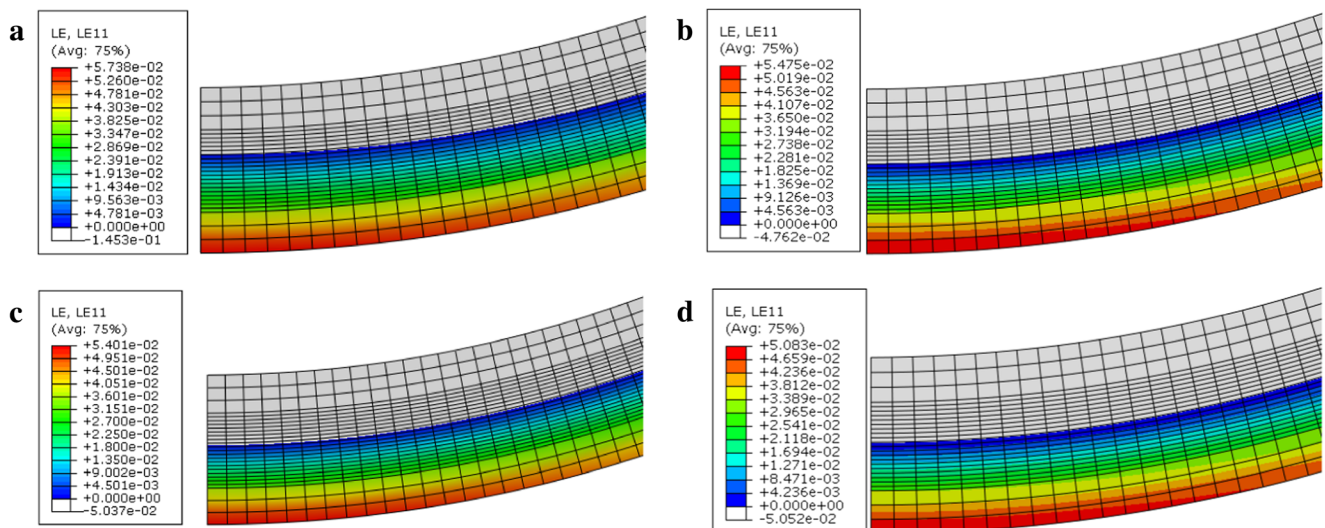


Fig. 12 Transverse strain distributions of **a** AA1060-polypropylene sandwich sheet, **b** AA5052-polypropylene sandwich sheet, **c** AA2024-polypropylene sandwich sheet, and **d** monolithic layer 5052 aluminum alloy sheet

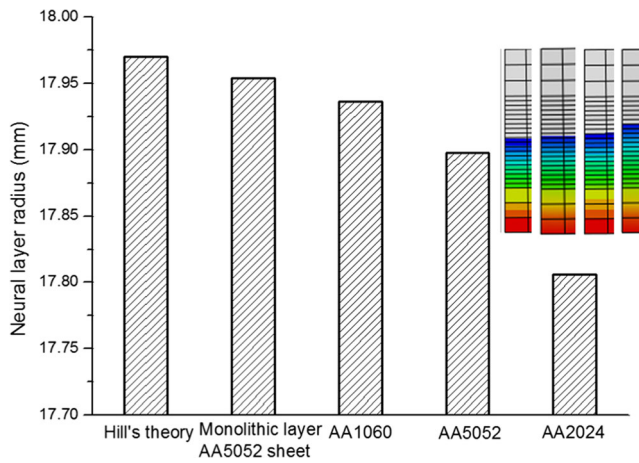


Fig. 13 Neutral layer radii for sandwich sheets and monolithic layer AA5052 sheet

alloy sheet, the influence of core polymer strength on the location of neutral layer becomes more obvious.

3. Thickness ratio of skin sheet to core materials

Thickness ratio of skin sheet to core materials is an important structure parameter for sandwich sheet. In order to investigate the influence of thickness ratio of skin sheet to core materials on the location of neutral layer, a relative neutral layer radius was defined as

$$\Phi = R_n / R_{Al}, \tag{27}$$

where R_n is the neutral layer radius of sandwich sheet obtained from simulations and R_{Al} is the neutral layer radius of monolithic layer aluminum alloy sheet with same thickness to sandwich sheet calculated according to Hill's theory.

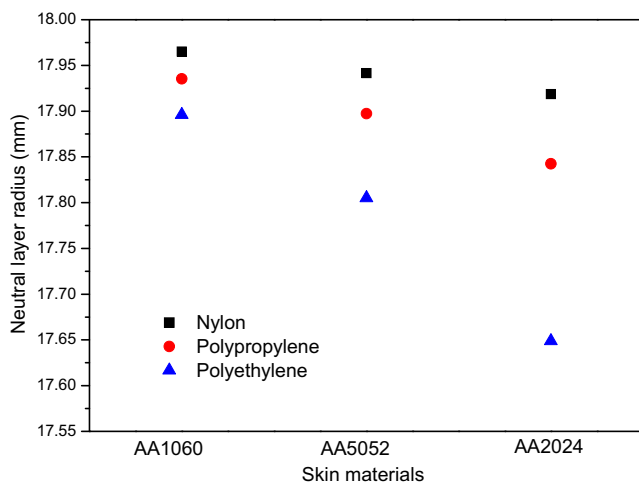


Fig. 14 Neutral layer radii for sandwich sheets

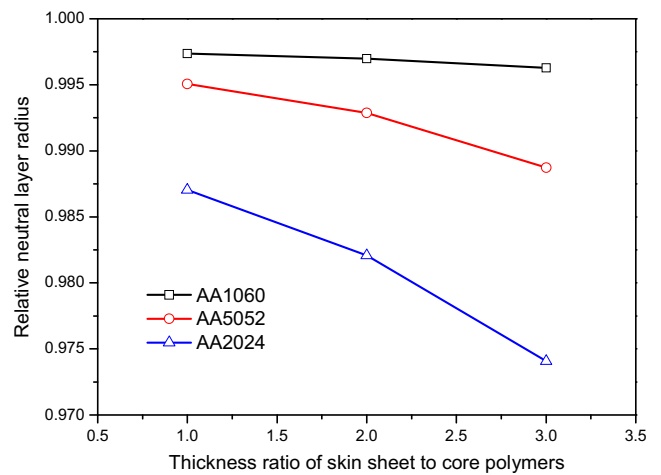


Fig. 15 Relative neutral layer radius with thickness ratio of skin sheet to core polymer

Figure 15 shows the influence of thickness ratio of skin sheet to core polymer on relative radius of neutral layer. With increasing thickness ratio of sandwich sheet, the relative neutral layer radius decreases and namely, the location of neutral layer shifts to compression region. The influence of thickness ratio of sandwich sheet on the location of neutral layer becomes more obviously with increasing strength of aluminum alloy sheet.

6 Springback behavior

6.1 Residual stress distribution

The transverse residual stress distributions of sheet part formed by bending will affect the loading capacity or the strength of the part. The transverse residual stress distributions

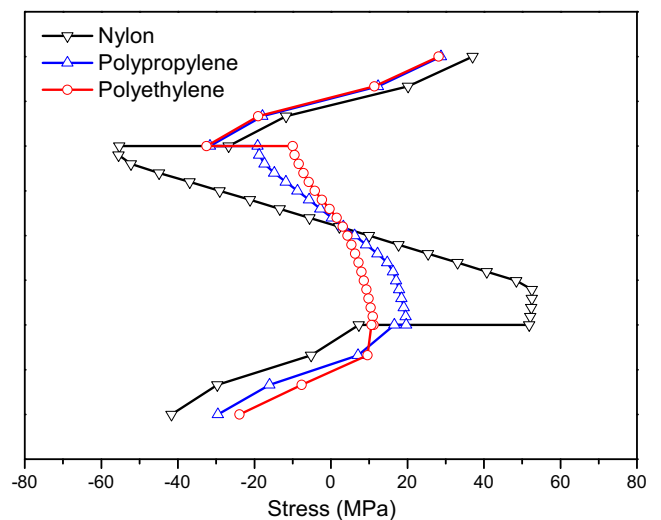


Fig. 16 Transverse residual stress distributions in sandwich sheets after springback

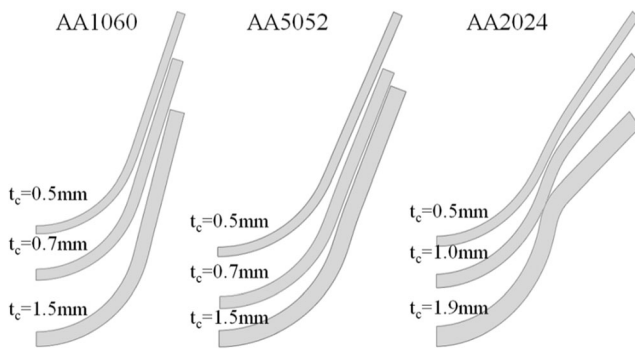


Fig. 17 Deformed geometries of bent specimens after springback

of AA5052-polymer sandwich sheets with three polymeric cores after springback are shown in Fig. 16. After unloading, the tension side of the bent specimen would have a significant compressive residual stress at the outer surface and there would be a residual tensile stress at the inner surface. The core polymer has little effect on the residual stress distributions of skin sheet.

6.2 Springback angle

1. Comparison of springback angle

The calculated, simulated, and experimental springback values were compared to verify the prediction capability of the proposed springback model and numerical simulation model. Figure 17 show the deformed geometries of bent specimens after springback. Figure 18 show comparisons of the measured and calculated springback angles. The springback angles calculated using the present analytical model was in fairly reasonable agreement with the experimental values despite the simplicity of our analytical approach. The simulated springback angle show little smaller than experimental ones.

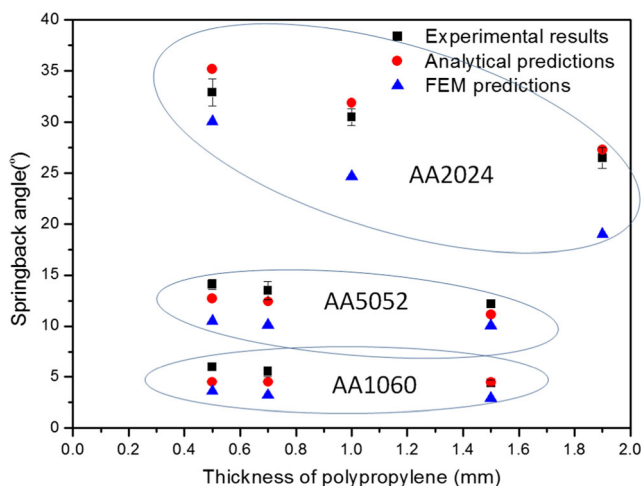


Fig. 18 Comparisons of calculated, simulated, and experimental springback angles

Table 4 Springback angle of sandwich sheet specimens

| Core material | | Skin aluminum sheet | | |
|---------------|---------------|---------------------|--------|--------|
| Thickness | Polymer | AA1060 | AA5052 | AA2024 |
| 0.5 | Polyethylene | 1.346 | 5.105 | 15.064 |
| | Polypropylene | 0.777 | 5.722 | 14.802 |
| | Nylon | 1 | 5.099 | 14.398 |
| 1.0 | Polyethylene | 1.608 | 5.047 | 12.345 |
| | Polypropylene | 1.039 | 4.78 | 11.549 |
| | Nylon | 0.999 | 4.097 | 11.103 |
| 1.5 | Polyethylene | 1.44 | 4.165 | 10.247 |
| | Polypropylene | 1.1 | 3.772 | 9.503 |
| | Nylon | 0.91 | 3.773 | 8.739 |

2. Influence of sandwich structure on springback angle

In Table 4, the springback angles of bent specimens were summarized. The springback angle decreases with increasing thickness of sandwich sheet, which is consistent with monolithic layer aluminum alloy sheet. But the influence of thickness on the springback angle relates to the skin aluminum alloy. When the skin sheet is 1060 aluminum alloy, the springback angle is very small and the thickness of sandwich sheet has not obviously effect on the springback angle. When the skin sheet is 2024 aluminum alloy, however, the springback angle is very large and the thickness of sandwich sheet has a significant effect on the springback angle.

For sandwich sheet with different skin sheets, the springback angle shows a great difference. When the skin sheet is 2024 aluminum alloy, the springback angle of sandwich sheet is far larger than other two aluminum alloy sandwich sheets. The springback angle increases with increasing strength of skin aluminum alloy sheet.

Core polymer has a slight effect on the springback angle of sandwich sheet. For sandwich sheet with same thickness and skin sheet, the springback angle increases with decreasing strength of core polymer. So, the springback angle of sandwich sheet is mainly determined by skin sheet.

7 Conclusions

In the present study, a simplified analytical model for springback prediction of sandwich sheet was proposed through analyzing the strain and stress distributions of skin sheet and core materials. Experiments and numerical simulations of unconstrained bending process for aluminum-polymer sandwich sheets were carried out. Folding defects, neutral layer position, and stress distributions during bending; residual stress distributions; and springback angle after

unloading were analyzed. The main conclusions from this work are given below:

1. The analytical predictions of springback angle have good agreements with experimental one.
2. The folding angle relates to the strength difference between the skin sheet and the core polymer. If the strength difference is larger, the folding angle is bigger. The folding angle also increases with the thickness of sandwich sheet.
3. Compared with monolithic layer aluminum alloy sheet, the neutral layer of sandwich sheet shifts to compression region. The neutral layer radius decreases with increasing strength of aluminum alloy sheet and decreasing strength of core polymer.
4. The springback angle of sandwich sheet increases with increasing strength of skin aluminum alloy sheet and the springback angle of sandwich sheet mainly depend on mechanical properties of the skin sheet.

Acknowledgements The authors would like to thank the National Natural Science Foundation of China (no. 50805034) and the Fundamental Research Funds for the Central Universities (no. HIT.NSRIF.2009033) for the support given to this research.

References

1. Miller WK (1980) Metal-plastic laminates for vehicle weight reduction. In: SAE International Congress, Detroit, SAE paper no. 800077. doi:10.4271/800077
2. Dicello JA (1980) Steel-polypropylene-steel laminate—a new weight reduction material. In: SAE International Congress, Detroit, SAE paper no. 800078. doi:10.4271/800078
3. Yao H, Chen CC, Liu SD, Li KP, Du C, Zhang L (2003) Laminated steel forming modelling techniques and experimental verifications. In: SAE International Congress, Detroit, SAE paper no. 2003-01-0689. doi:10.4271/2003-01-0689
4. Veenstra EW (1993) Aluminum-plastic-aluminum sandwich sheet for maximum weight reduction in body panels. In: SAE International Congress, Detroit, SAE paper no. 930706. doi:10.4271/930706A
5. Shin KS (1999) Mechanical properties of aluminum/polypropylene/aluminum sandwich sheets. *Met Mater Int* 5:613–618. doi:10.1007/BF03026313
6. Kim KJ, Kim D, Choi SH, Chung K, Shin KS, Barlat F, Oh KH, Youn JR (2003) Formability of AA5182/polypropylene/AA5182 sandwich sheets. *J Mater Process Tech* 139:1–7. doi:10.1016/S0924-0136(03)00173-0
7. Compston P, Cantwell WJ, Cardew-Hall MJ, Kalyanasundaram S, Mosse L (2004) Comparison of surface strain for stamp formed aluminum and an aluminum-polypropylene laminate. *J Mater Sci* 39:6087–6088. doi:10.1023/B:JMSC.0000041707.68685.72
8. Liu J, Liu W, Xue W (2013) Forming limit diagram prediction of AA5052/polyethylene/AA5052 sandwich sheets. *Mater Design* 46:112–120. doi:10.1016/j.matdes.2012.09.057
9. Parsa MH, Ettehad M, Matin PH (2013) Forming limit diagram determination of Al 3105 sheets and Al 3105/polypropylene/Al 3105 sandwich sheets using numerical calculations and experimental investigations. *J Eng Mater-T Asme* 135:031003. doi:10.1115/1.4023848
10. Kim KJ, Rhee MH, Choi BI, Kim CW, Sung CW, Han CP, Kang KW, Won ST (2009) Development of application technique of aluminum sandwich sheets for automotive hood. *Int J Precis Eng Man* 10:71–75. doi:10.1007/s12541-009-0073-5
11. Makinouchi A, Yoshida S, Ogawa H (1988) Finite element simulation of bending process of steel–plastic laminate sheets. *J JSTP* 29:755–760
12. Huang YM, Leu DK (1995) Finite-element simulation of the bending process of steel/polymer/steel laminate sheets. *J Mater Process Tech* 52:319–337. doi:10.1016/0924-0136(94)01617-A
13. Parsa MH, Ettehad M, Matin PH, Ahkami SN (2010) Experimental and numerical determination of limiting drawing ratio of Al3105-polypropylene-Al3105 sandwich sheets. *J Eng Mater-T Asme* 132:031004. doi:10.1115/1.4001264
14. Lee MG, Kim JH, Chung K, Kim SJ, Wagoner RH, Kim HY (2009) Analytical springback model for lightweight hexagonal close-packed sheet metal. *Int J Plasticity* 25:399–419. doi:10.1016/j.ijplas.2008.04.005
15. Lee MG, Kim D, Wagoner RH, Chung K (2007) Semi-analytic hybrid method to predict springback in the 2D draw bend test. *J Appl Mech-T Asme* 74:1264–1275. doi:10.1115/1.2745390
16. Li K, Carden WP, Wagoner RH (2002) Simulation of springback. *Int J Mech Sci* 44:103–122. doi:10.1016/S0020-7403(01)00083-2
17. Bahloul R, Ayed LB, Potiron A, Batoz JL (2009) Comparison between three optimization methods for the minimization of maximum bending load and springback in wiping die bending obtained by an experimental approach. *Int J Adv Manuf Tech* 48:1185–1203. doi:10.1007/s00170-009-2332-0
18. Lepadatu D, Hambli R, Kobi A, Barreau A (2005) Optimisation of springback in bending processes using FEM simulation and response surface method. *Int J Adv Manuf Tech* 27:40–47. doi:10.1007/s00170-004-2146-z
19. Ito K, Kasajima M, Furuya S (1981) Bending and spring back theory of metal–polymer sandwich laminates. *J Macromol Sci B* 19:773–791. doi:10.1080/00222348108246321
20. Liu L, Wang J (2004) Modeling springback of metal-polymer-metal laminates. *J Manuf Sci Eng-T Asme* 126:599. doi:10.1115/1.1765141
21. Yuen WYD (1996) A generalised solution for the prediction of springback in laminated strip. *J Mater Process Tech* 61:254–264. doi:10.1016/0924-0136(95)02182-5
22. Corona E, Eisenhour T (2007) Wiping die bending of laminated steel. *Int J Mech Sci* 49:392–403. doi:10.1016/j.ijmecsci.2006.08.007
23. Li HB, Chen J, Yang J (2012) Experimental and numerical investigation of laminated steel sheet in V-bending process considering nonlinear visco-elasticity of polymer layer. *J Mater Process Tech* 212:36–45. doi:10.1016/j.jmatprotec.2011.08.002
24. Parsa MH, Mohammadi SV, Aghchai AJ (2014) Al3105/polypropylene/Al3105 laminates springback in V-die bending. *Int J Adv Manuf Tech* 75:849–860. doi:10.1007/s00170-014-6173-0
25. Mohammadi S, Parsa M, Aghchai AJ (2014) Simplified springback prediction in Al/PP/Al sandwich air bending. *J Sandw Struct Mater* 17:217–237. doi:10.1177/1099636214560580
26. Parsa MH, Ahkami SNA, Ettehad M (2010) Experimental and finite element study on the spring back of double curved aluminum/polypropylene/aluminum sandwich sheet. *Mater Design* 31:4174–4183. doi:10.1016/j.matdes.2010.04.024
27. Weiss M, Dingle ME, Rolfe BF, Hodgson PD (2007) The influence of temperature on the forming behavior of metal/polymer laminates in sheet metal forming. *J Eng Mater-T Asme* 129:530–537. doi:10.1115/1.2772329